Electronic Supplementary Material (ESI) for Energy & Environmental Science

The Structure and Activation of Substrate Water Molecules in the S_2 State of Photosystem II Studied by Hyperfine Sublevel Correlation Spectroscopy.[†]

Sergey Milikisyants,[1] Ruchira Chatterjee,[1] Christopher S. Coates,[1] Faisal H. M. Koua,[2] Jian-Ren Shen[2] & K. V. Lakshmi[1]

[1]Department of Chemistry and Chemical Biology and

The Baruch ’60 Center for Biochemical Solar Energy Research

Rensselaer Polytechnic Institute

Troy, NY 12180

[2]Division of Bioscience

Graduate School of Natural Science and Technology and Faculty of Science

Okayama University

Okayama 700-8530, Japan

TITLE RUNNING HEAD: Two-Dimensional ^{14}H HYSCORE Spectroscopy of the S_2 State of Photosystem II.

[†]This study is supported by the Photosynthetic Systems Program, Office of Basic Energy Sciences, United States Department of Energy (DE-FG02-07ER15903).

Supporting Information

*Author for Correspondence:

K. V. Lakshmi

Department of Chemistry and Chemical Biology

Rensselaer Polytechnic Institute

Troy, NY 12180

Phone: (518) 276 3271

Fax: (518) 276 4887

Email: lakshk@rpi.edu

Key Words: Photosystem II, solar water oxidation, S_2 state, tetra-nuclear manganese calcium-oxo (Mn_4Ca-oxo) cluster, EPR spectroscopy, HYSCORE spectroscopy, ESEEM spectroscopy.

2D HYSCORE Spectroscopy.

Qualitative Analysis of the 2D ^{1}H HYSCORE Spectra.

In the form of two-dimensional cross-correlation peaks, 2D HYSCORE spectroscopy measures the energy splittings of the electron spin manifolds that are induced by the electron-nuclear hyperfine interaction with a magnetic nucleus. In disordered powder samples, the cross-peaks appear as extended ridges as the intensity is distributed over a certain region in the 2D frequency space. In the case of protons (nuclear spin I = 1/2), for each nucleus there are two ridges that are symmetric with respect to the main diagonal of the 2D space. The isotropic component of the electron-nuclear hyperfine interaction that arises from a Fermi contact interaction results in an increased separation between the ridges which shifts each ridge away from the main diagonal (the diagonal is defined as a straight line determined by equation $\nu_1 + \nu_2 = 0$). The anisotropic component of the hyperfine interaction that is caused by a through space dipolar interaction results in the extension of the ridges which increases the area covered by the ridges and simultaneously shifts the ridges from the anti-diagonal (the anti-diagonal is defined by the equation $\nu_1 + \nu_2 = 2\nu_Z$, where $\nu_Z = 14.37$ MHz). Thus, we identify five distinct pairs of ridges in the 2D ^{1}H HYSCORE spectra that are shown in Figure 3, Figure 3S and Figure 4S.

Quantitative Analysis of the 2D ^{1}H HYSCORE Spectra.

The three principal components of an electron-nuclear hyperfine tensor can be presented as:

$$(A_x, A_y, A_z) = (a_{iso} - T(1 - \delta), a_{iso} - T(1 + \delta), a_{iso} + 2T) \quad (1)$$

where a_{iso}, T, and δ are the isotropic, dipolar, and rhombic components of the tensor, respectively. In the case of axial symmetry ($\delta = 0$, $A_x = A_y = A_\perp = a_{iso} - T$, $A_z = A_\parallel = a_{iso} + 2T$), the proton cross-peaks (which appear as ridges in powder samples) represent straight line segments when plotted in frequency-squared coordinates.[1] A frequency-squared plot of the 2D ^{1}H HYSCORE spectrum of the S_2 state of the OEC in *T. vulcanus* is shown in Figure 6S. All of the ridges that are observed in the frequency-squared plot have a linear shape that is relatively narrow. This indicates the presence of axially symmetric hyperfine interactions. In this case, the anisotropic and isotropic components of the electron-nuclear hyperfine interaction can be obtained from the slope and the intercept of the ridges.[2] Based on the values of the slope, $Q_{\alpha(\beta)}$, and the intercept, $G_{\alpha(\beta)}$, that are determined experimentally, the values of a_{iso} and T can be calculated from following equations:[3]

$$T = \pm\sqrt{\frac{16}{9(1-Q_{\alpha(\beta)})}\left\{G_{\alpha(\beta)} + \frac{4\nu_I^2 Q_{\alpha(\beta)}}{1-Q_{\alpha(\beta)}}\right\}} \text{ and } a_{iso} = \pm 2\nu_I \frac{1+Q_{\alpha(\beta)}}{1-Q_{\alpha(\beta)}} - \frac{T}{2} \qquad (2)$$

To obtain the values $Q_{\alpha(\beta)}$ and $G_{\alpha(\beta)}$, the frequency-squared coordinates of the points were measured on the median of a ridge corresponding to the highest signal intensity along the direction of the ridges. The measured coordinates were then subjected to a linear fit using a least squares algorithm which yielded the values of $Q_{\alpha(\beta)}$ and $G_{\alpha(\beta)}$.

In principle, each pair of $Q_{\alpha(\beta)}$ and $G_{\alpha(\beta)}$ values results in four sets of possible hyperfine parameters (please see equation (2)), where, the sign of T can be positive or negative and for a given value of T, there are two possible values of a_{iso}. The numerical simulations cannot be reliably used to discriminate among the four possibilities, since microwave pulse imperfections distort the 2D HYSCORE intensity distribution over the ridges. Such imperfections are very hard

to account for in numerical analysis. However, the right parameter set can be selected based on the electronic properties of the paramagnetic center. Table 1S lists four sets of hyperfine values for a_{iso} and T for five groups of protons, H^{I} - H^{V}, that are determined in this study. Usually the value of T is positive, since it is a through-space dipolar interaction. However in a cluster of four manganese ions, the sign of the dipolar interaction is determined by the spin projection factors of each of the manganese ions. Thus both positive and negative signs are possible. The selection can be based on the highly ionic nature of a metal-ligand bond for the high-valence manganese centers. This results in the delocalization of the electron spin density from the metal ion. Previous experimental and theoretical hyperfine studies of mixed valence Mn(III)-Mn(IV) model complexes indicate that the absolute values of a_{iso} should not exceed ~ 3 MHz.[4] More importantly, the value of a_{iso} should either be very small (< 1 MHz) or the sign of a_{iso} should be the same as the sign of T. Thus, we reject all of the sets of hyperfine parameters for which a_{iso} is considerably larger than this limit. We also reject the values of a_{iso} where the sign is different than the sign of T. Using these selection criteria, we obtain two sets of hyperfine parameters for four groups of protons, H^{I} - H^{IV}. We cannot discriminate between the four sets, corresponding to two signs of T and two different values of a_{iso} for H^{V}. Nevertheless, we conclude that for the H^{V} group of protons, the absolute value of a_{iso} of ~ 2 MHz is highly improbable, since a very small value of T of ± 1.4 MHz indicates that H^{V} cannot be located in close proximity of any of the metal ions. Thus, H^{V} should have very small value of a_{iso}. The final list of hyperfine parameters for H^{I} - H^{V} are presented in Table 1 of the main text.

To estimate the errors of the hyperfine parameters, the admissible variation of values of the slope and the intercept, $Q_{\alpha(\beta)}$ and $G_{\alpha(\beta)}$, were estimated by considering various points in the middle of the ridges and the variation amplitude of the hyperfine parameters was taken as its error bar.

Numerical Simulations of the 2D ^{1}H HYSCORE Spectra.

As a final test of the validity of the hyperfine parameters that were obtained by linear analysis, numerical simulations of the spectra were performed using the "saffron" function of the EasySpin software package and the numerical simulations were compared with the experimental spectra.[5] The simulated 2D ^{1}H HYSCORE spectrum of the S_2 state of the OEC of PSII from *T. vulcanus* was numerically calculated using the set of hyperfine parameters in Table 1 of the main text (Figure 7S). The major spectral features of the simulated spectrum and the position of the ridges in the 2D frequency space are in excellent agreement with the experimental spectrum (Figure 3). This confirms the validity of the hyperfine parameters that are obtained in this study. The minor visual differences between the experimental and simulated spectra are due to the inability of the simulation to describe imperfections of the microwave pulses that lead to differences in the distribution of the signal intensity of the ridges.

Deuterium Exchange Experiments on the S_2 State of Photosystem II.

In order to obtain a better understanding of the nature of the groups of protons, H^{I} - H^{V}, that display hyperfine interactions in the S_2 state of the OEC we exchanged the PSII samples in D_2O buffers. In the PSII samples where the protons are replaced by deuterons, we observe significant suppression of the intensity of the cross-peaks in the ^{1}H HYSCORE spectra of the S_2 state. Figure 8S shows a comparison of the skyline projections of the S_2 state of the OEC in *T. vulcanus* in H_2O buffer (blue trace) and after 6 hours of D_2O exchange (red trace). The residual intensity of the ^{1}H HYSCORE cross-peaks is ~ 30% of the initial value. A similar effect is observed for spinach PSII that is exchanged in D_2O buffer for 3 hours and 24 hours (Figure 9S).

The intensity of the ^{1}H HYSCORE signals in Figure 9S are also suppressed to ~ 30% when spinach PSII is exchanged in D_2O buffer. This could indicate the replacement of the exchangeable protons in the OEC by deuterons. However, it is important to consider that the decrease of the ^{1}H HYSCORE signals could also be caused by cross suppression effects that are known to occur in ESEEM and HYSCORE spectroscopy due to the presence of very strong modulations arising from other nuclei. Thus, the suppression of the proton cross-peaks that is observed in the ^{1}H HYSCORE spectra does not provide reliable confirmation that the five groups of protons, H^{I} - H^{V}, are exchangeable as cross suppression might be the dominating effect upon deuterium exchange. In addition, the presence of intense modulations arising from the matrix deuterons and the poor signal-to-noise ratio of the cross-peaks in the ^{1}H HYSCORE spectra of PSII that is exchanged in D_2O buffer precludes reliable analysis of the proton hyperfine interactions. However, ^{2}H HYSCORE spectroscopy could provide important information with respect to the exchangeable deuterons in the vicinity of the Mn_4Ca-oxo cluster in the S_2 state of the OEC. The ^{2}H HYSCORE spectroscopy experiments of the S_2 state are currently in progress.

REFERENCES.

1. S. A. Dikanov and M. K. Bowman, *J. Magn. Reson., Ser. A*, 1995, **116**, 125.

2. S. A. Dikanov, R. I. Samoilova, D. R. J. Kolling, J. T. Holland and A. R. Crofts, *J. Biol. Chem.*, 2004, **279**, 15814.

3. A. M. Weyers, R. Chatterjee, S. Milikisiyants and K. V. Lakshmi, *J. Phys. Chem. B*, 2009, **113**, 15409.

4. D. W. Randall, M. K. Chan, W. H. Armstrong and R. D. Britt, *Mol. Phys.*, 1998, **95**, 1283.

5. S. Stoll and A. Schweiger, *J. Magn. Res.*, 2006, **178**, 42.

TABLES.

Table 1S. The hyperfine interaction parameters of the ^{1}H nuclei obtained by linear analysis of the 2D ^{1}H HYSCORE spectrum of the S_2 state of PSII from *T. vulcanus* (Figure 3 of the main text).

Table 1S.

Ridge	T, MHz	a_{iso}, MHz
H^{I}	4.4 -4.4	1.8, -4.4 -1.8, 4.4
H^{II}	4.1 -4.1	0.1, -4.1 -0.1, 4.1
H^{III}	1.9 -1.9	2.6, -4.5 -2.6, 4.5
H^{IV}	2.3 -2.3	0.2, -2.5 -0.2, 2.5
H^{V}	1.4 -1.4	0.5, -2.0 -0.5, 2.0

FIGURE CAPTIONS:

Figure 1S. The 2D ^{1}H HYSCORE spectrum of the S_2 state of PSII from the PsbB variant of *Synechocystis* PCC 6803 at g = 1.95 with τ = 176 ns.

Figure 2S. The skyline projection plot of the 2D ^{1}H HYSCORE spectrum of the S_1 state and S_2 state of PSII from the PsbB variant of *Synechocystis* PCC 6803 at g = 1.95 with (A) τ = 140 ns and (B) τ = 176 ns.

Figure 3S. The (-, +) and (+, +) quadrants of the 2D HYSCORE spectrum of (A) S_2 and (B) S_1 state of PSII from the PsbB variant of *Synechocystis* PCC 6803.

Figure 4S. The 2D ^{1}H HYSCORE spectrum of the S_2 state of PSII from the PsbB variant of *Synechocystis* PCC 6803 at g = 1.95 with τ = 140 ns.

Figure 5S. The 2D ^{1}H HYSCORE spectrum of the S_2 state of PSII membranes from spinach at g = 1.95 with τ = 140 ns.

Figure 6S. The frequency-squared representation of the 2D ^{1}H HYSCORE spectrum of the S_2 state of PSII from *T. vulcanus* at g = 1.95 with τ = 140 ns.

Figure 7S. The numerical simulation of the experimental 2D ^{1}H HYSCORE spectrum of the S_2 state of PSII from *T. vulcanus* using the parameter set in Table 1 at g = 1.95 with τ = 140 ns.

Figure 8S. The skyline projection plots of the 2D HYSCORE spectrum of the S_2 state of PSII from *T. vulcanus* at g = 1.95 in H_2O buffer (blue) and exchanged for 6 hours in D_2O buffer (red).

Figure 9S. The skyline projection plots of the 2D HYSCORE spectrum of the S_2 state of spinach PSII at g = 1.95 in H_2O buffer (black), exchanged for 3 hours (red) and 24 hours (blue) in D_2O buffer.

Figure 1S

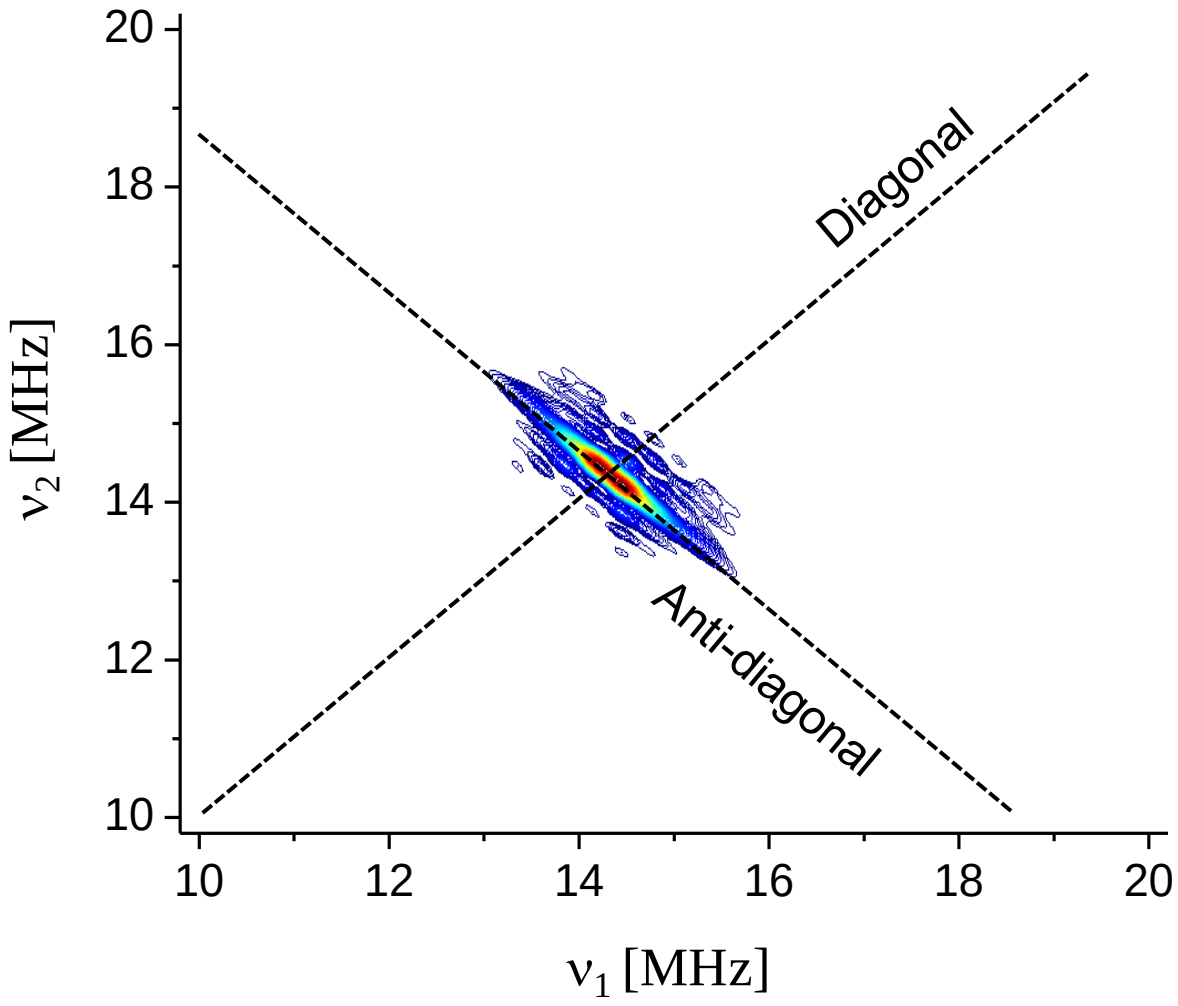

Figure 2S.

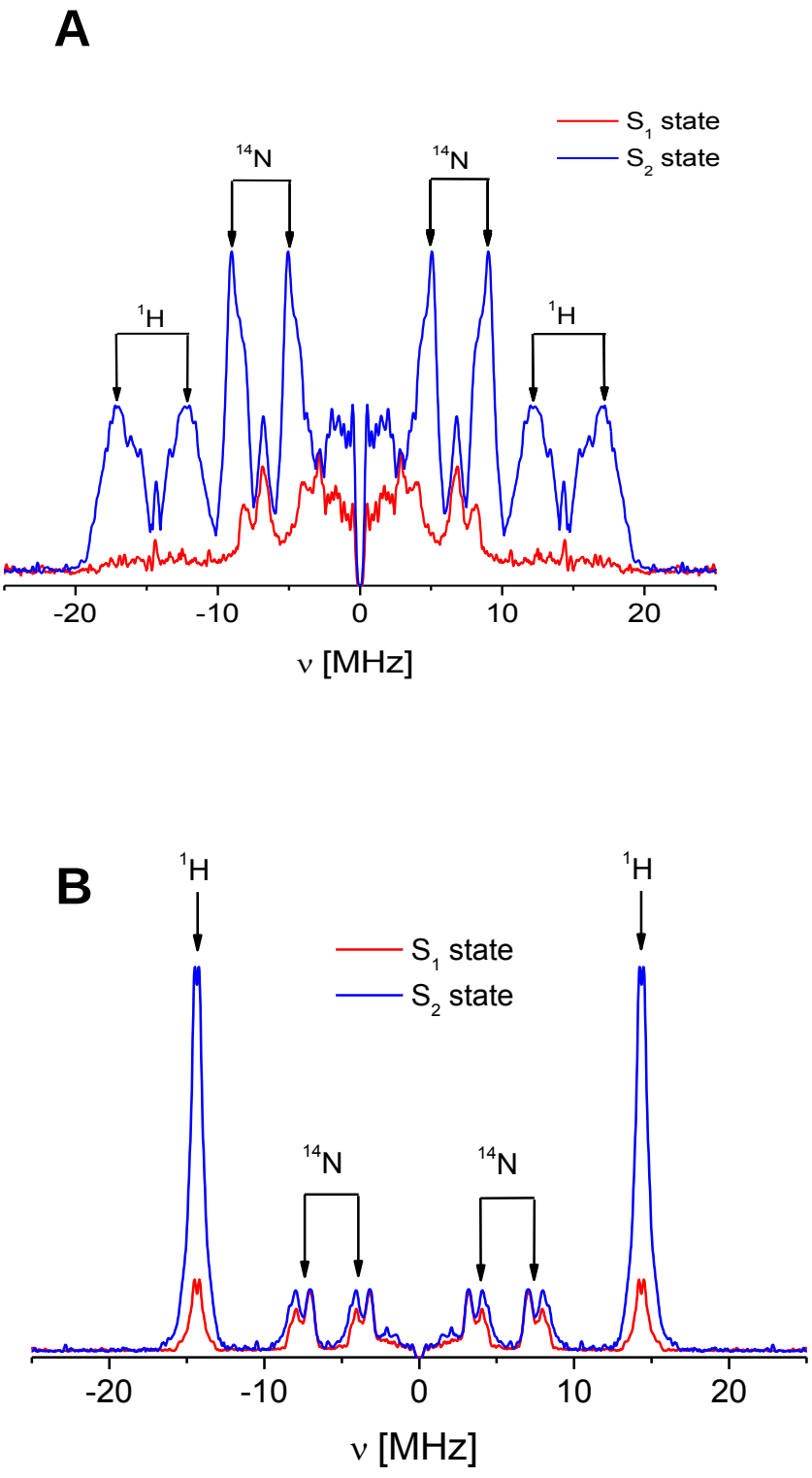

Figure 3S.

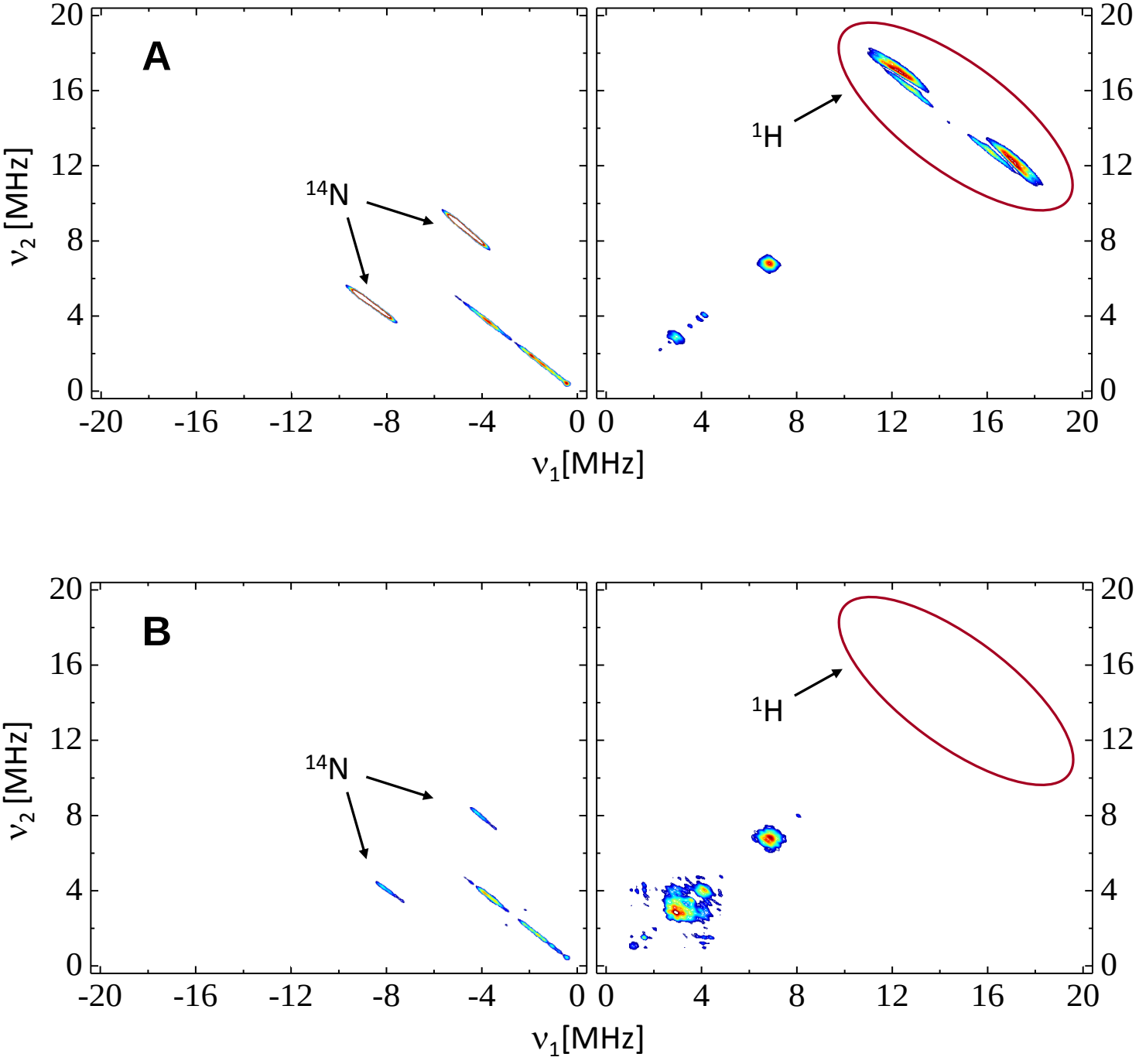

Figure 4S

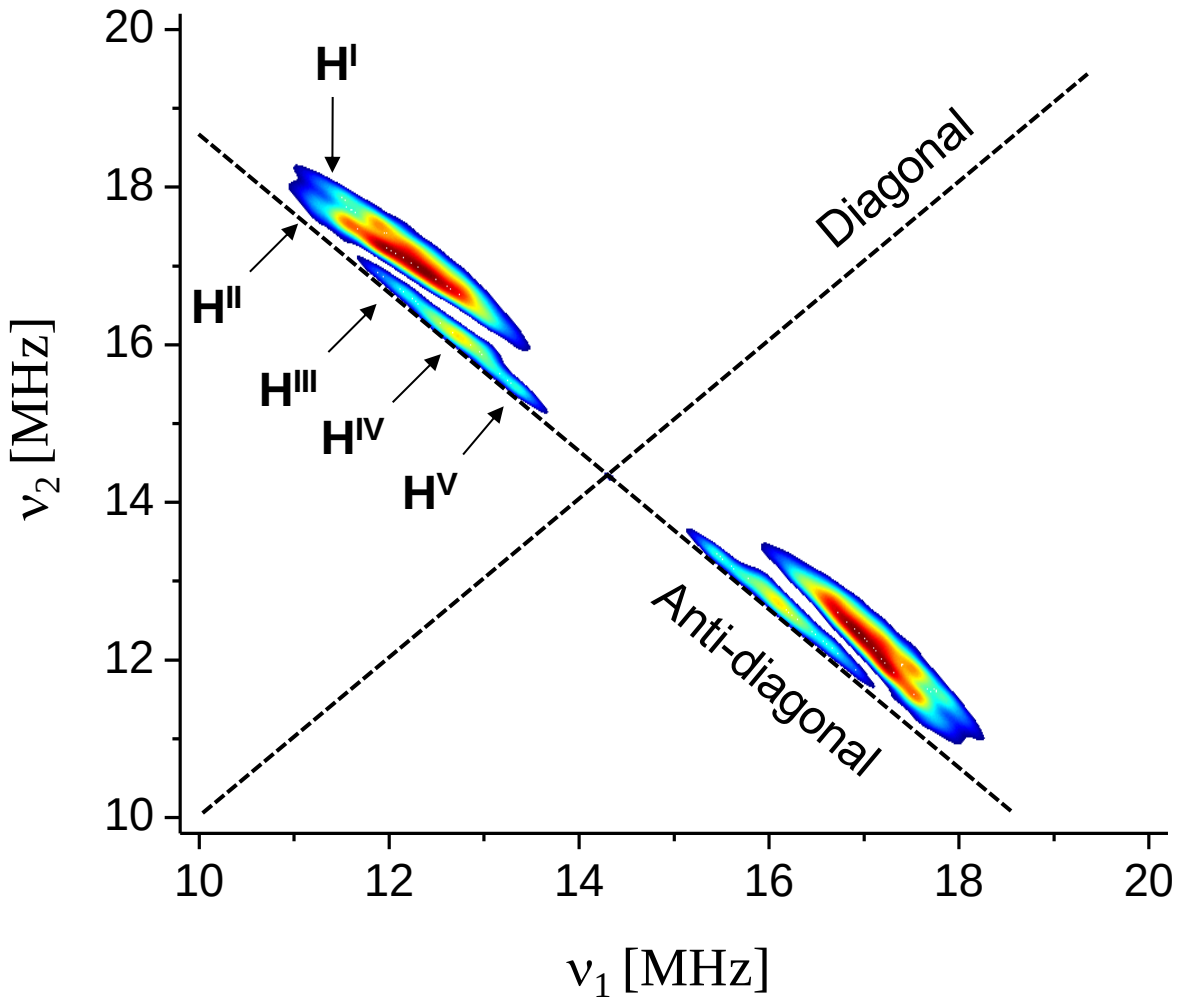

Figure 5S

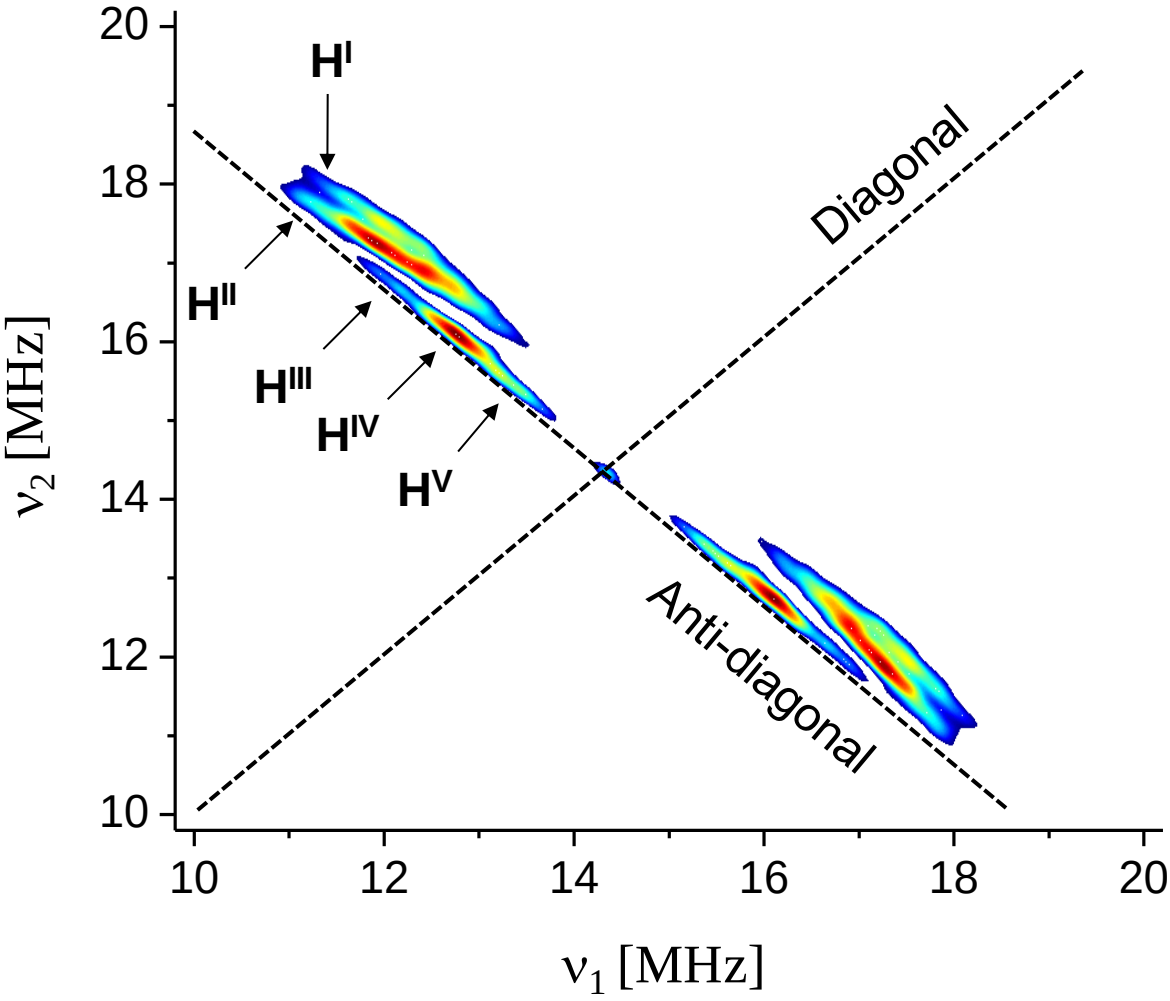

Figure 6S.

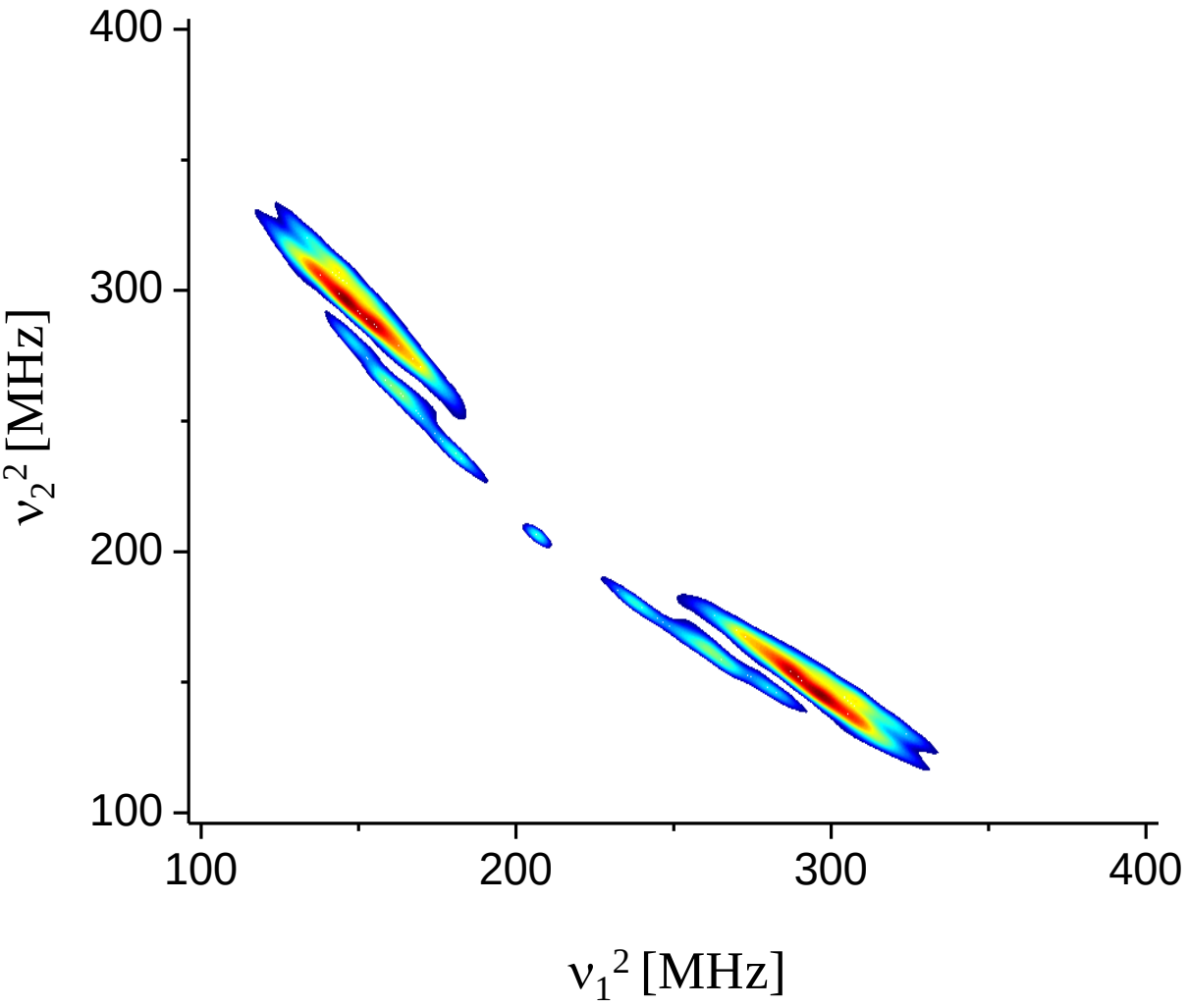

Figure 7S.

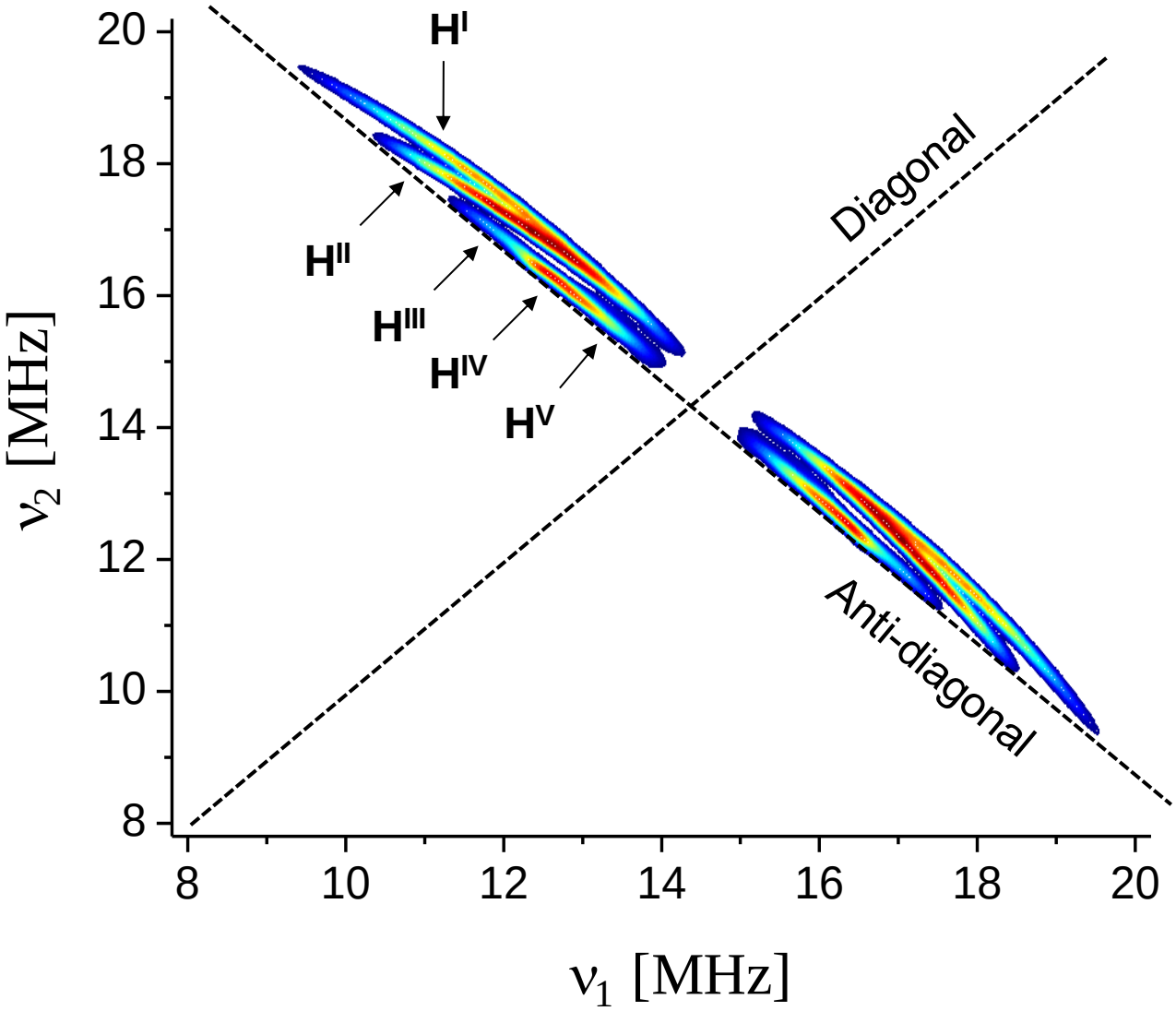

Figure 8S.

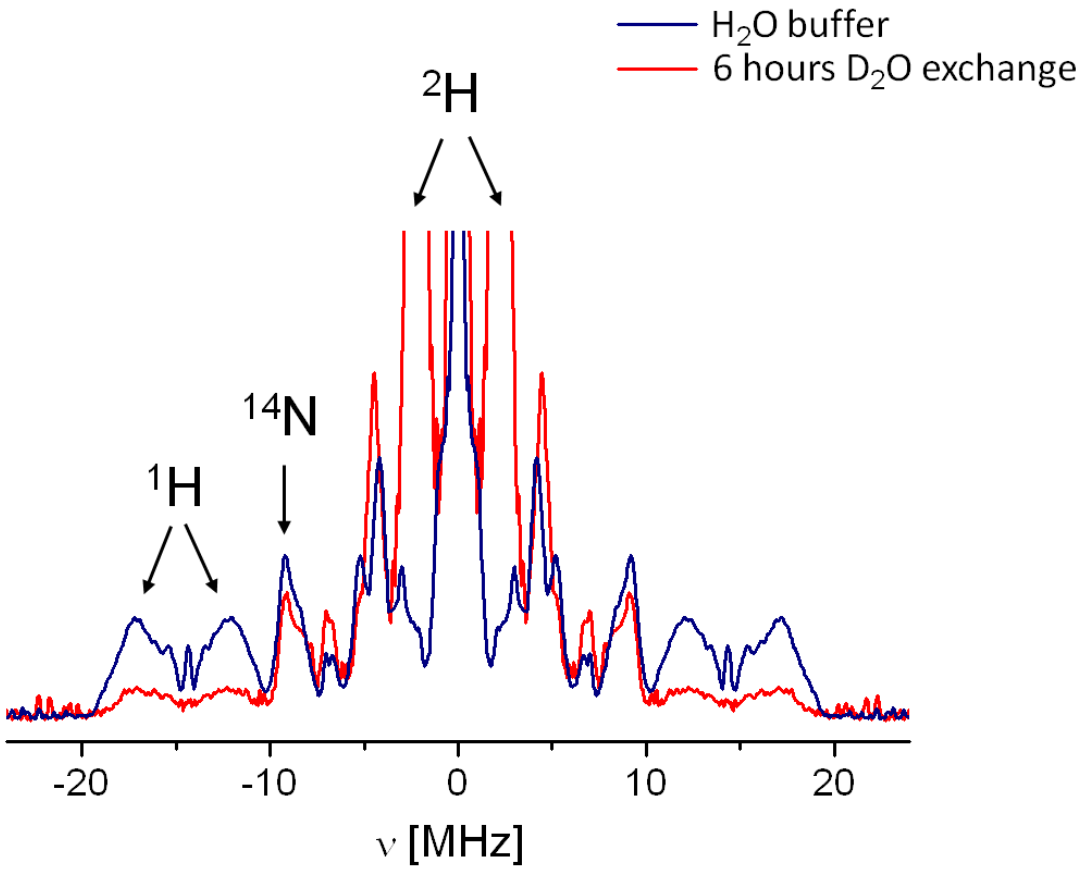

Figure 9S.